This is the peer reviewd version of the followng article:

Modeling and optimization of industrial internal combustion engines running on Diesel/syngas blends / Rinaldini, C.A., Allesina, G., Pedrazzi, S., Mattarelli, E., Tartarini, P.. - In: ENERGY CONVERSION AND MANAGEMENT. - ISSN 0196-8904. - 182:(2019), pp. 89-94. [10.1016/j.enconman.2018.12.070]

Terms of use:

The terms and conditions for the reuse of this version of the manuscript are specified in the publishing policy. For all terms of use and more information see the publisher's website.

07/11/2026 20:37

(Article begins on next page)

*Revised Manuscript with no changes marked
Click here to view linked References

Modeling and optimization of industrial internal combustion engines running on Diesel/syngas blends

Carlo Alberto Rinaldini[a], Giulio Allesina[a], Simone Pedrazzi[a,*], Enrico Mattarelli[a], Paolo Tartarini[a]

[a] University of Modena and Reggio Emilia, Department of Engineering 'Enzo Ferrari',
Via Vivarelli 10/1, 41125 Modena, Italy

[*] Corresponding author, email address: simone.pedrazzi@unimore.it

Abstract

The paper presents a numerical analysis of combustion, carried out on a compression ignition indirect injection engine fueled by both Diesel and syngas, the latter obtained from biomass gasification and introduced in the intake manifold. The computational fluid dynamics model includes an improved chemical kinetics scheme, tailored on the syngas-diesel dual fuel combustion. The model was validated by an experimental campaign, on the same engine. The syngas fuel was produced by a small scale gasifier running on wood chips. Several simulations were performed varying both the share of syngas and the Diesel start of injection angle. The total amount of heat released by combustion can increase up to 50%, along with the indicated work and the cylinder peak pressure. The start of injection angle should be modified in order to preserve the mechanical integrity of the engine, as well as to maximize its brake efficiency. The numerical analysis provides the guidelines for setting the injection strategy, as a function of the syngas share.

Keywords: biomass, gasification, diesel, dual-fuel, combustion.

1 INTRODUCTION:

Today great attention is paid to renewable sources as sustainable alternative to fossil fuel for energy production and transport. In 2016, about 500 TWh of electrical energy was generated from biomass, accounting for 2% of world electricity generation, while transport biofuels provided 4% of world road transport fuel demand. A study of the International Energy Agency reports that biofuels can provide up to 27% of world transportation fuel by 2050 and bioenergy will provide nearly 17% of final energy demand in 2060 [1]. One of the most promising propositions, especially in stationary industrial and agricultural applications, is the partial replacement of diesel fuel with syngas, as an example when running internal combustion engines for electricity production [2]. Syngas is a gaseous mixture obtained through solid fuel gasification, it is mainly composed of carbon monoxide (CO), hydrogen (H_2), carbon dioxide (CO_2), nitrogen (N_2), methane (CH_4). The proportion between these constituents depends on the process, reactor architecture and the type of solid fuel [3]. Among the different

technologies for syngas production, biomass gasification is one of the most promising. Small scale power plants generally rely on internal combustion engines for the final energy conversion of the gaseous fuel into mechanical and then electrical power. The system complexity can range from simple open top reactors to multi-stage gasifiers [4]. On a worldwide literature scale, Susastriawan et al. [5] reviewed the most common technologies used for small scale gasification, while Patuzzi et al. focused on the northern part of Italy [6]. The Compression Ignition (CI) engine is the most obvious candidate for burning syngas, due to its intrinsic high efficiency and robustness [7]. When operated in dual fuel (DF) mode, CI engines show a reduction of diesel oil fuel consumption and of particulate matter emissions. This was observed in the experimental tests for syngas use in oleaginous-based power plants [8], in syngas-Balanites aegyptiaca ester oil blends [9]. Effects of Diesel substitution were observed also in single-cylinder engines [10]. In this work, a Kohler KDW 1404, 4-cylinder, indirect injection engine is considered. The engine is modeled by means of a CFD-3D code (KIVA-3V), in order to analyze the simultaneous combustion of diesel oil and syngas under several operating conditions. The use of CFD allows for an in-depth sight of the combustion process revealing details that cannot be easily measured with more expensive experimental tests. Moreover, numerical simulations allows for the analysis of a large number of configurations and making reliable comparisons thanks to the possibility of varying one parameter at the time while boundary conditions are keep strictly constant. However, the engine model used in this work had been previously calibrated on the base of experimental campaign results [8], where the engine was coupled to a commercial fixed bed gasifier produced by All Power Labs (model PP10) [11]. As far as the CFD analysis is concerned, particular attention is paid to the dual fuel combustion process, requiring the modeling of a series of complex phenomena: liquid fuel injection, droplets atomization and vaporization, mixing of Diesel vapor within the air-syngas premixed environment and ignition. For the optimization of dual combustion, two fundamental parameters are varied: syngas-diesel share and the Diesel injection advance. The choice of these two parameters is motivated by the possibility to easily tune them in almost any type of Diesel engine, employed in stationary applications. Starting from a previously validated standard diesel combustion model, a flame propagation model was implemented and added to simulate the combustion process in a dual fuel regime. Results show a strong dependence of combustion patterns on the share of energy substitution from Diesel oil to syngas. At some operating points, the syngas-supported combustion enables a noticeable increase of engine brake efficiency. On the other hand, an excess of syngas leads to undesired high values of peak pressure within the combustion chamber. The CFD simulation results provide a comprehensive overview on the influence of both the start of injection angle (SOI) and the share of syngas. Assuming a maximum peak cylinder pressure value of 100 bar, a correlation between the optimum SOI and the share of syngas is extrapolated. Obviously, the optimum SOI corresponds to the maximum brake efficiency of the engine, while complying with the constraint on combustion pressure. The limit of 100 bar is based on the authors experience, as well as on the results of a previous comprehensive

experimental campaign on the same Kohler engine running on standard Diesel oil. The measured parameters are also employed as a reference for the calibration of the CFD-3D engine model. Particular attention is obviously paid to the combustion process. The calibrated model is then applied to the investigation of a broad range of operating conditions in order to map the effects of combined variations of syngas-Diesel share and start of injection timing. The use of CFD analysis allows to investigate conditions where the peak pressure may exceed the maximum value suggested by the engine manufacturer.

2 MATERIALS AND METHODS

Compression ignition engines always require a minimum amount of Diesel fuel, in order to inject the premixed air-syngas charge. In many cases, the substitution rates can be pushed up to 90-95% [12], however in this work the substitution range is limited to 60% of the fuel total chemical energy. A further increase was experimentally demonstrated to produce unacceptable peaks of cylinder gas pressures (over 150 bar), therefore the 60% limit was set in order to preserve the mechanical integrity of the engine.

2.1 Gasification and engine facility

The syngas composition input used in the modeling of the systems derives from the analysis of the producer gas obtained during the experimental tests that lead also to model calibration. During the experimental campaign, the Kohler KDW 1404 engine was connected to a gasification unit model Power Pallet PP10 manufactured by All Power Labs [11]. The Power Pallet is a complete power-delivery system equipped with a gas generation reactor, a filtration stage composed of a cyclone and a woodchips packed-bed drum filter and an engine-generator unit that consists in a model DG972 3-cylinder Kubota engine. For the experimental run the whole generator unit was disconnected and the filtered gas directly sent to the compression ignition engine instead. The gasification reactor is a fixed bed, single throat, Imbert-type gasifier fed from the top through an auger connected to a 63 liters fuel-storage hopper. For the experimental campaign dry poplar wood chips were used as fuel. After a start-up period of about 20 minutes where the gas was burned in a flare, the gas composition resulted stable with little or no dependency on the flow rate required by the engine. This feature characterizes the Imbert-type gasifiers, it was vital in the past for variable load application such as vehicle propulsion, and it is known in classic literature as ‘turn down ratio’ as reported in the FAO “Wood Gas as an Engine Fuel” book [13] and in the Reed’s gasification handbook [14]. The gasification facility description, as reported by the manufactured, is summarized in Table 1. During the tests the gasifier behavior was proven to be stable, combustion temperature set itself to 920 °C, while the temperature

at the end of the reduction zone was 770 °C. The composition analysis of the produced gas was performed through two tests run in a Pollution 3000 Micro-GC gas analyzer. The lower heating value of the syngas is calculated as follows:

$$LHV_{syngas} = LHV_{H_2} x_{H_2} + LHV_{CO} x_{CO} + LHV_{CH_4} x_{CH_4} \quad (1)$$

where LHV_{syngas} [MJ/Nm^3] is the syngas lower heating value; LHV_{H_2}[MJ/Nm^3] is the hydrogen lower heating value (10.8 MJ/Nm^3 [15]); x_{H_2} [% mol] is hydrogen molar fraction in the syngas; LHV_{CO} [MJ/Nm^3] is the carbon monoxide lower heating value (12.6 MJ/Nm^3 [15]); x_{CO} [% mol] is carbon monoxide molar fraction in the syngas; LHV_{CH_4}[MJ/Nm^3] is the methane lower heating value (35.9 MJ/Nm^3 [15]) and x_{CH_4} [% mol] is methane molar fraction in the syngas. About the IC engine, a 4-cylinder Kohler KDW 1404, with indirect injection [16] was used in an engine test bench described by the authors [8]. Some engine features reported in Table 2 indicate the highly robustness and reliability of this engine, which is normally used in industrial and agricultural applications.

Table 1 APL PP10 features [11].

Parameter	**Value**
Power output	from 3 to 10 kW electrical power
Maximum biomass consumption	12 kg/h @ 10 kWel
Fuel moisture tolerance	up to 30% moisture content
Dimensions (LxWxH)	1.2 x 1.2 x 1.8 m
Weight	499 kg

Table 2 Kohler KDW 1404 features [16]

Parameter	**Value**
Cylinders	4-in line
Total displacement	1372 cm^3
Bore	75 mm
Stroke	77.6 mm
Compression ratio	22.8:1
Injection system	Indirect injection with injector dump on head
Applications	Excavator, dumper, roller, generation set

2.2 Gas flow rate measurement and control

During the calibration tests the engine run under two different conditions in terms of syngas-Diesel share. Unlike other systems on the market where an air blower push air into the reactor to generate a specific amount of gas, the system chosen works below atmospheric pressure. It is the engine that draws gas from the reactor and through the filtration stage. For the calibration tests the same architecture of the original generator was used: the diesel engine air intake was connected to the reactor using a tee as shown in Figure 1. Due to the pressure drop generated by the gasifier-filter system, air will always find its way into the open branch of the tee. For this reason, acting on the air valve placed in this branch, the engine is forced to draw both gas and air. A differential pressure meter, connected to a calibrated orifice in the gas branch keeps records of the gas flow rate thanks to the following equation:

$$Q_m = \frac{C}{\sqrt{1-\beta^4}} \varepsilon \frac{\pi d^2}{4} \sqrt{2\rho_1 \Delta p} \quad (2)$$

where C is the coefficient of discharge, β is the ratio between the pipe and the orifice diameters, d is the orifice diameter, ρ_1 is the fluid density, as function of the temperature, ΔT is the differential pressure across the plate, ε is the expansibility factor, calculated as follows:

$$\varepsilon = 1 - (0.41 + 0.35\beta^4) \frac{\Delta p}{k \cdot p_1} \quad (3)$$

where k is the heat capacity ratio, p_1 is the upstream pressure.

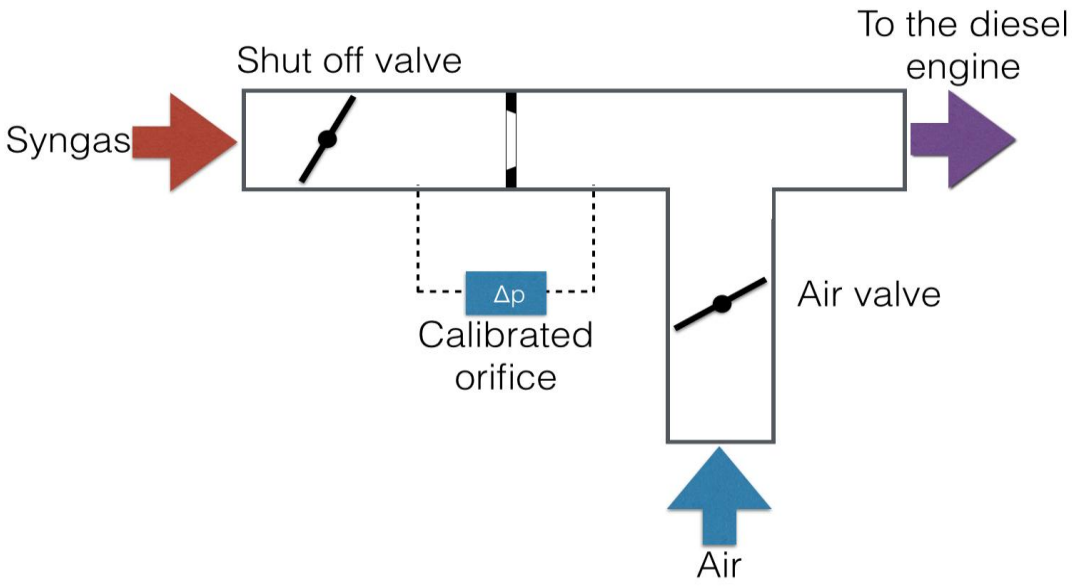

Figure 1 Syngas-air mixing system (adapted from [8])

2.3 Computational Fluid Dynamic Model

The CFD model used in this work is based on the KIVA-3V code, customized for the purposes of the study. In particular, a specific chemical kinetic sub-model is implemented for the investigation of the syngas-diesel dual fuel (DF) operations. A list of the most important sub-models employed in the customized version of the KIVA 3V code is shown in Table 3.

Table 3 Description of the modeling environment

Modeling Environment	**Description**
Turbulence model	RNG k-H
model Breakup	model Hybrid KH-RT
model Droplet collision	model Droplet trajectories
Evaporation model	Single component, KIVA-3V
Diesel Combustion	PaSR / coupled chemical kinetics
Flame Propagation	TFC / Premix code for aspirated fuel
Fuel composition	Syngas/DOS

Most of the sub-models mentioned in Table 3 were widely used by the authors within KIVA-3V and KIVA 4 environments, so a detailed description of their implementation can be found in previous works. For example, Mattarelli et al. [17] applied the KIVA CFD model to light duty Dual Fuel (Diesel/Natural Gas) combustion engine. The model is able to predict the emission formation as reported by Golovitchev at al. [18]. In addition, the model was used to simulate 2-stroke engines [19] and Miller cycle diesel engine [20]. The present paper only reviews the modeling of syngas-Diesel simultaneous combustion. This goal is achieved thanks to the synergy between two different sub-models. The first one, typically employed for standard Diesel operations, is the partially premixed reactor spray combustion model, PaSR, [21]; the second is a specific flame propagation model. For the latter, the authors implemented a new expression for the reaction rate. The development and validation of the chemical kinetic mechanisms were carried out with the support of experiments: ignition delay times measured in shock tubes, for different natural gas/diesel premixed charge compositions and flame propagation data for the main constituent components of natural gas. The

mechanism tuning methodology used in this study was based on a sensitivity analysis of complex mechanisms and it is comprehensively described in [22].

Before the investigation on the Dual Fuel operations, a CFD-3D model of the engine cylinder was built and validated by comparison with experimental data, for both Normal Diesel (ND) and Diesel-syngas Dual Fuel (DF) combustion. The computational grid cannot be shown due to not-disclosure agreements; it was generated to accurately reproduce the geometric details of the combustion chamber, to achieve the actual compression ratio and to get a good aspect ratio of cells. The typical cell size is about 0.5-1.0 mm and a minimum of 4 cell layers was enforced in the squish region at Top Dead Center. As demonstrated in previous analyses [18], experimentally validated in [23], these meshing criteria guarantee a good compromise between accuracy and computational demand. The computational grid consists of about 100,000 cells at BDC and of about 20,000 at TDC.

Initial conditions for combustion simulations, such as pressure, temperature, trapped mass and charge composition, were obtained from experimental data, while in-cylinder initial velocity was imposed on the basis of the authors' experience. However, this arbitrary hypothesis should have a negligible influence on combustion, since the hyper turbulence imparted by the pre-chamber is supposed to prevail on any variation of the in-cylinder initial flow field.

3 RESULTS AND DISCUSSION

Both experimental and CFD results show a strong dependence on engine in-cylinder pressure and overall efficiency on the share of Diesel substitution.

3.1 Calibration tests

Syngas sampling results are reported in Table 4. Data show a negligible variability among the samples. The calculated average gas composition is 6 MJ/Nm^3. This value is in agreement with the recorded behavior of downdraft fixed bed reactors [3,4].

Table 4 Syngas composition

	x_{H_2} [% mol.]	x_{N_2} [% mol.]	x_{CH_4} [% mol.]	x_{CO} [% mol.]	x_{CO_2} [% mol.]	LHV_{syngas} [MJ/Nm^3]
Sample 1	20.3	45.2	1.8	25.0	7.6	5.99
Sample 2	20.3	45.3	1.8	25.1	7.5	6.00
Average	20.3	45.3	1.8	25.1	7.6	6.00

Combustion simulation results were compared to experiments for 2 operating points: the first is an ND operation, full load, 3000 rpm and the second was derived from the first, reducing the injected Diesel fuel of about 38% and replacing it with the amount of syngas that enables the engine to generate the same brake power. Table 5 reports the details of each operating point while Figure 2 shows the comparison between predicted and measured in-cylinder pressure. As visible, for both ND and DF operations, close agreement with experiments was found. From the data in Table 4 and from Figure 2, it can be also seen that DF combustion yields a slight increase of engine brake efficiency (+2.3%) but also leads to an increment in in-cylinder peak pressure (about 8 bar). The same tendency was observed in a previous work by Rinaldini et al. [2], where a Common Rail 2.8 liter, turbocharged Diesel engine, fueled by both syngas and Diesel, was tested at the dynamometer bench. Here, a slightly higher brake efficiency increment of 5 % was measured at a diesel substitution rate of 27 %

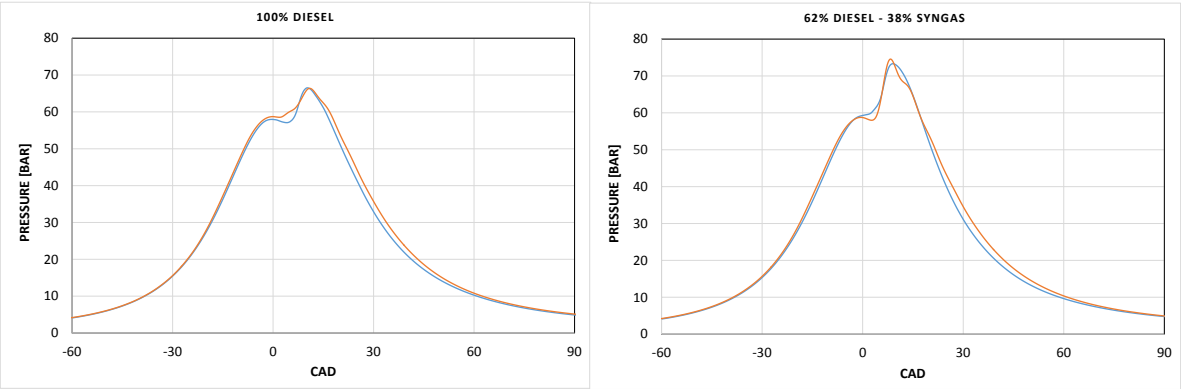

Figure 2 Model Validation

Table 5 Engine operating point used for the model validation

		ND	DF
Rotational speed	rpm	3000	3000
Power	kW	15.65	15.65
Diesel flow rate	l/h	5.40	3.35
Diesel fuel power	kW	54.45	33.78
Syngas flow rate	Nm^3/h	0.00	11.67
Syngas fuel power	kW	0.00	19.45

Engine brake efficiency	%	28.74	29.40

3.2 Model results

In order to analyze DF combustion, a set of CFD-3D simulations were performed, by using the calibrated models and varying both syngas premixed concentration and Diesel injection strategies. In detail, the amount of injected Diesel fuel was progressively reduced and substituted with premixed syngas; for each DF simulated case, the amount of syngas was calculated, according to Eq. 4, in order to keep the ND case equal to the total amount of energy introduced with the two fuels. The Diesel Replacement Rate (DRR) parameter, defined in Eq. 5, was used to identify the substitution levels. Finally, the Start of Injection (SOI) of Diesel fuel (-4 CAD ATDC for base engine) was varied from -8 CAD ATDC to 2 CAD ATDC.

$$m_{syngas,DF} = (m_{Diesel,ND}k_{i,Diesel} - m_{Diesel,DF}k_{i,Diesel})/k_{i,syngas} \quad (4)$$

$$DRR = (m_{Diesel,ND} - m_{Diesel.DF})/m_{Diesel,ND} \quad (5)$$

In order to evaluate the indicated work, directly related to the engine power output, the Gross Indicated Mean Effective Pressure (IMEP*) is calculated as the pressure-volume integral from -60° to 110° after firing TDC, divided by the engine unit displacement. Figures 3 and 4 are the maps of total heat released by combustion and IMEP*; these parameters are plotted as a function of the syngas fraction (corresponding to DRR) and start of injection (SOI). The solid lines crossing the maps represent the iso-values of maximum in-cylinder pressure, reached for each combination of DRR and SOI. It is important to notice that these results cannot be directly compared to the ones previously presented for the model validation, since they are obtained under different conditions (same engine power output for the calibration results, same fuel input energy for the current ones).

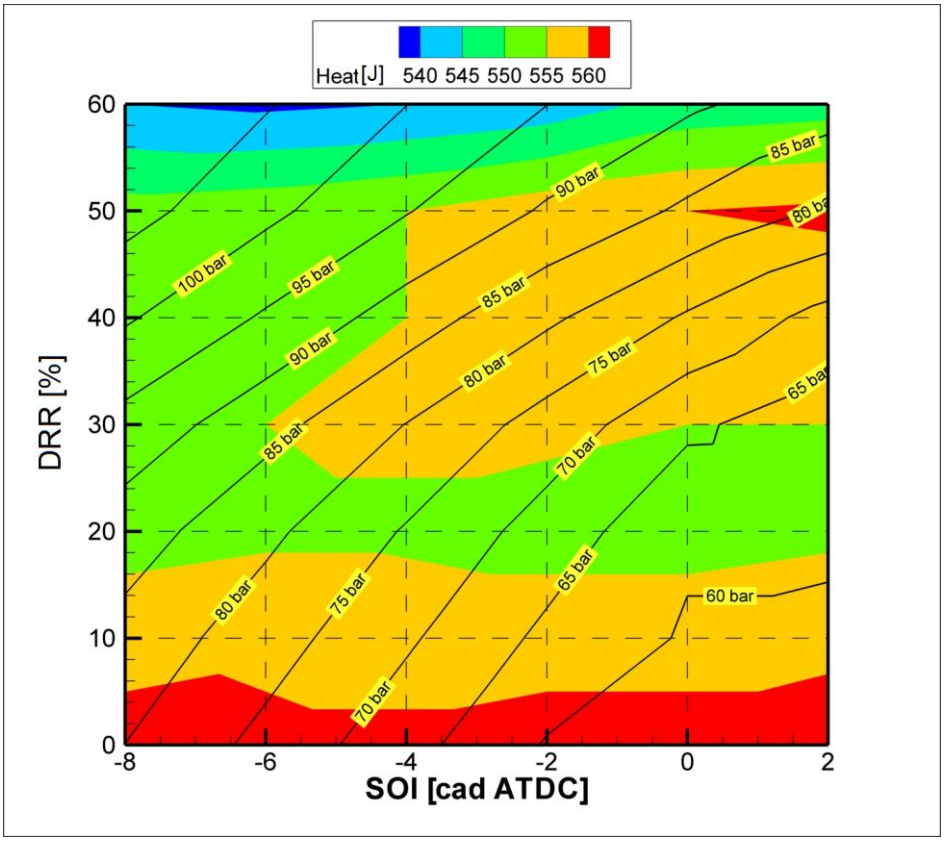

Figure 3 Modeled combustion heat release Vs. DRR and SOI

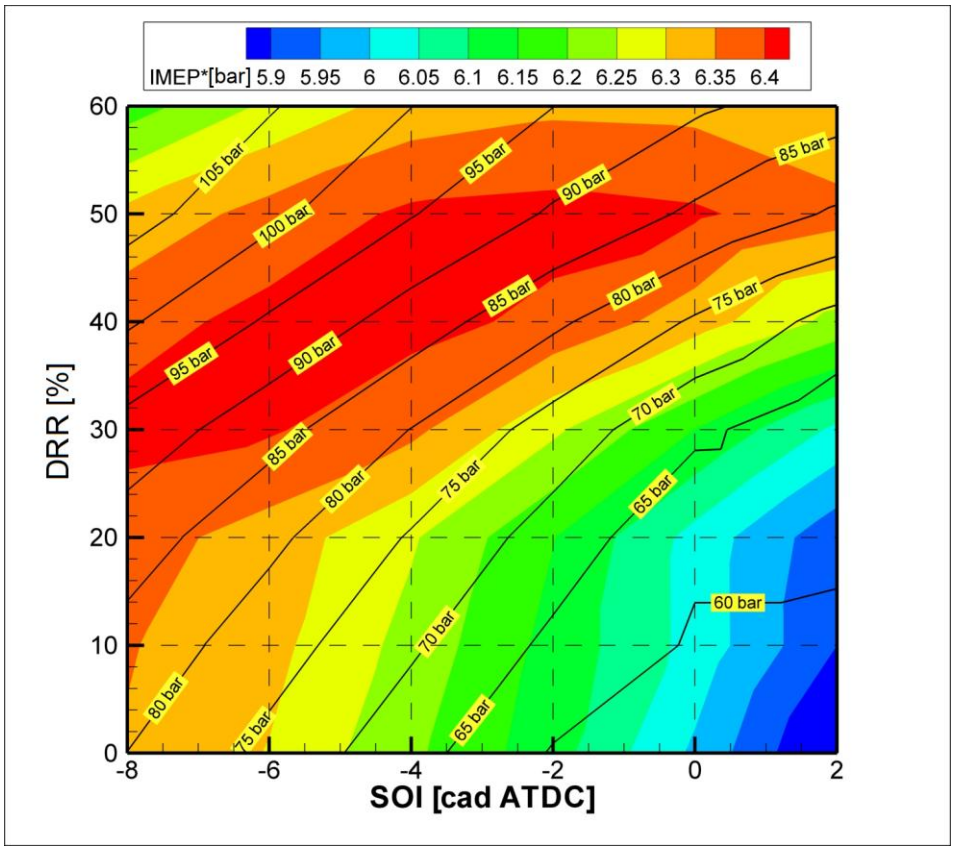

Figure 4 Modeled IMEP* Vs. DRR and SOI

Looking at Figure 3 and 4, the following considerations can be made.

- Combustion heat release slightly decreases as DRR increases; however, variations are quite small (max 4%), indicating that combustion efficiency is more or less the same over the map. As a result, engine indicated efficiency depends almost entirely on the efficiency of the conversion of heat into work: therefore, the higher is IMEP*, the higher will be the engine fuel conversion efficiency.
- As expected, earlier injections correspond to larger IMEP* but also to higher in-cylinder pressures (in-cylinder peak pressure iso-lines and IMEP* bands have approximately the same shape); moreover, as DRR increases, IMEP* and peak pressures increase.
- Considering a limit for peak cylinder pressure of 100 bar, it may be observed from figure 4 that any rate of substitution from 10 to 60% can yield a value of IMEP* higher than in the ND operation, while complying with the above mentioned constraint. This means that dual fuel operations may improve the brake performance and efficiency of the engine (1-5%), without drawbacks in terms of mechanical stress on the cylinder components.
- For DRR higher than 50%, there is a drop in the IMEP* values, even if the in-cylinder peak pressure continues to increase: a possible explanation for this result may be the slight reduction of combustion efficiency, demonstrated in Figure 3 by the fall of released heat.

3.3 Optimization of the engine brake efficiency

From the analysis of figures 4 and 5 it is also possible to determine a correlation between the Diesel substitution rate (DRR), and the SOI angle, that maximizes the engine brake efficiency, while complying with the above mentioned limit of 100 bar for the peak cylinder pressure. For the same level of efficiency, the SOI angle that provides minimum cylinder pressure was chosen. The results of this post-processing activity are presented in figure 5. For this set of data, a second degree polynomial interpolation curve was calculated:

$$SOI\ [cad\ ATDC] = 0.0013DRR^2 + 0.094DRR - 8.9406 \quad (6)$$

The coefficient of determination (R^2) is 0.9134. The scattering of points in Figure 5 that does not allow the definition of a higher degree polynomial monotonic function. Eq. 6 can be used as a basis for defining the injection strategy of all the engines of the same type, simultaneously operating with syngas and Diesel.

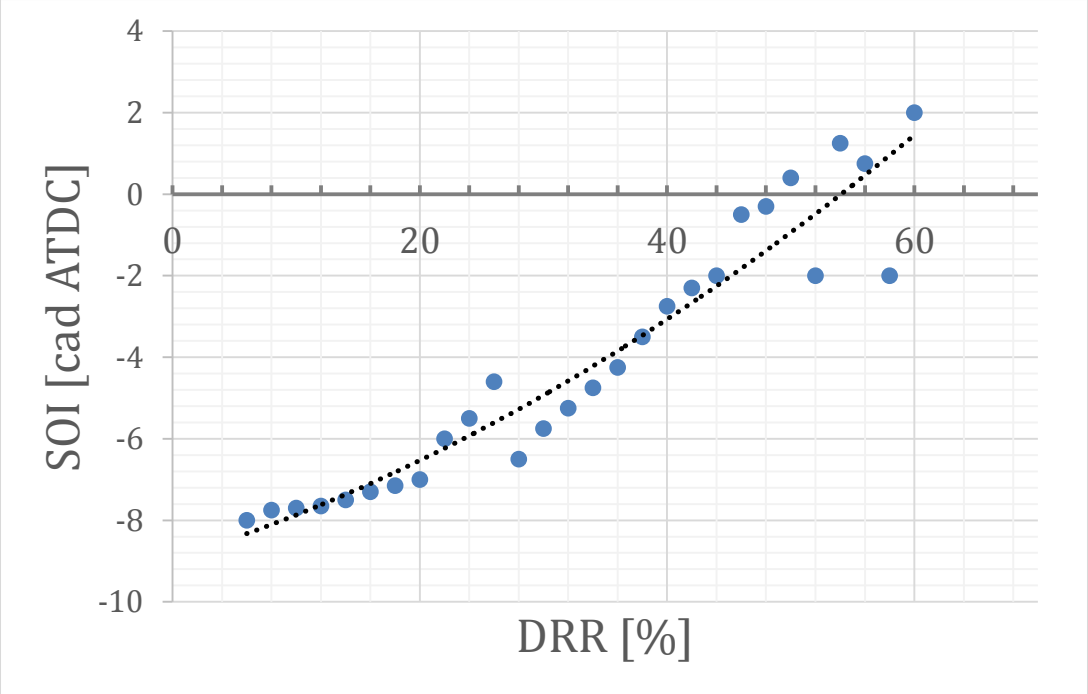

Figure 5 SOI-DRR correlation for maximizing engine brake efficiency

4 CONCLUSIONS

A CFD-3D combustion analysis of a 1.4 liter, 4-cylinder, IDI industrial Diesel engine was carried out, using a KIVA-3V model, validated by experiments. Two types of combustion were investigated: a conventional Diesel combustion (ND), and a dual fuel (DF) combustion, where the Diesel fuel is partially replaced by syngas. The maximum rate of substitution considered in the study is 60%. The main goal of the study was to analyze the influence of the injection strategy, as well as to assess the potential of this dual fuel combustion in terms of engine performance and brake efficiency.

It was found that for substitution rates up to 40-50% engine performance and efficiency can increase a little bit (1-5%), however it is fundamental to properly set the injection angle, in order to control peak cylinder pressure. In order to achieve the maximum fuel efficiency, while complying with the pressure limit, a correlation between optimum SOI and the replacement rate was calculated. This function can be applied also to different engines, of the same type. Dual fuel combustion of Diesel and syngas was demonstrated to be an effective way to exploit renewable energy sources, with minimum modifications to the existing engines.

Nomenclature

Acronym/abbreviation	Meaning
ATDC	After Top Dead Center
BDC	Bottom Dead Center
CAD	Crankshaft Angle Degrees
CFD	Computational Fluid Dynamics
CI	Compression Ignition
DF	Dual Fuel
DOS	Diesel Oil Surrogate
DRR	Diesel replacement rate
IC	Internal Combustion
IMEP	Indicated Mean Effective Pressure
KH-RT	Kelvin-Helmholtz Rayleigh-Taylor
LHV	Lower Heating Value
ND	Normal Diesel
PaSR	Partially Stirred Reactor
RNG	Renormalization Group
SOI	Start Of Injection
TDC	Top Dead Center
TFC	Turbulent Flame Closure

References

[1] OECD/IEA. Technology Roadmap - Delivering Sustainable Bioenergy, http://www.iea.org/publications/freepublications/publication/Technology_Roadmap_Delivering_Sustainable_Bioenergy.pdf [accessed 25 October 2018].

[2] Rinaldini CA, Allesina G, Pedrazzi S, Mattarelli E, Savioli T, Morselli N, Puglia M, Tartarini P. Experimental investigation on a Common Rail Diesel engine partially fuelled by syngas. Energy Conversion and Management 2017;138:526-537. https://doi.org/10.1016/j.enconman.2017.02.034.

[3] Basu P. Biomass Gasification, Pyrolysis and Torrefaction, Pratical Design and Theory. 3rd ed. London: Academic Press; 2018.

[4] De Sales CAVB, Maya DMY, Lora EES, Jaén RL, Reyes AMM, González AM, Andrade RV, Martínez JD. Experimental study on biomass (eucalyptus spp.) gasification in a two-stage downdraft reactor by using mixtures of air, saturated steam and oxygen as gasifying agents. Energy Conversion and Management 2017;145:314-323. https://doi.org/10.1016/j.enconman.2017.04.101.

[5] Susastriawan AAP, Saptoadi H, Purnomo. Small-scale downdraft gasifiers for biomass gasification: A review. Renewable and Sustainable Energy Reviews 2017; 76:989-1003. https://doi.org/10.1016/j.rser.2017.03.112.

[6] Patuzzi F, Prando D, Vakalis S, Rizzo AM, Chiaramonti D, Tirler W, Mimmo T, Gasparella A, Marco Baratieri. Small-scale biomass gasification CHP systems: Comparative performance assessment and monitoring experiences in South Tyrol (Italy). Energy 2016;112:285-293. https://doi.org/10.1016/j.energy.2016.06.077.

[7] Dasappa S, Sridhar HV. Performance of a diesel engine in a dual fuel mode using producer gas for electricity power generation, International Journal of Sustainable Energy 2013;32,3:153-168. https://doi.org/10.1080/14786451.2011.605945.

[8] Allesina G, Pedrazzi S, Rinaldini CA, Savioli T, Morselli N, Mattarelli E, Tartarini P. Experimental-analytical evaluation of sustainable syngas biodiesel CHP systems based on oleaginous crop rotation (Conference Paper). In: International conference on power engineering, ICOPE 2015; PACIFIC Yokohama Conference Center Yokohama; Japan; 30 November 2015 through 4 December 2015; Code 118770.

[9] Deshmukh SJ, Bhuyar LB, Thakre SB. Investigation on performance and emission characteristics of CI engine fuelled with producer gas and esters of Hingan (Balanites) oil in dual fuel mode. International Journal of Aerospace and Mechanical Engineering 2008;2,3:148-153.

[10] Mahgoub BKM, Sulaiman SA, Abdul Karim Za. Performance of a Compression Ignition Engine Fuelled by Diesel and Imitated Syngas. Asian Journal of Scientific Research 2013;6: 456-466

[11] ALL Power Labs. PP10 Power Pallet datasheet, http://www.allpowerlabs.com/ [accessed 25 October 2018].

[12] Kumar S, Date MA, Pandya RN, Patel S, Shah KC, Damour V, Jain BC. Design and Development of a Biomass Based Small Gasifier-Engine System Suitable for Irrigational Needs in Remote Areas of Developing Countries. In: Energy from Biomass and Wastes VIII; Institute of Gas Technology; Chicago; 1984.

[13] United Food and Agriculture Organization. Wood Gas as an Engine Fuel. Rome: FAO Forestry Paper; 1986.

[14] Reed TB, Das A. Handbook of Biomass Downdraft Gasifier Engine Systems. Golden (Colorado): Solar Energy Research Institute;1984.

[15] The Engineering Toolbox. Gross and Net Heating Values for some common Gases, Available at: https://www.engineeringtoolbox.com/gross-net-heating-values-d_420.html [accessed 25 October 2018].

[16] Kohler Power. KDW 1404 engine webpage, http://www.kohlerpower.it/product/kdw-1404/ [accessed 25 October 2018].

[17] Mattarelli E, Rinaldini CA, Golovitchev VI. CFD-3D analysis of a light duty Dual Fuel (Diesel/Natural Gas) combustion engine. Energy Procedia 2014;45:929–37. https://doi.org/10.1016/j.egypro.2014.01.098.

[18] Golovitchev VI, Rinaldini CA, Montorsi L, Rosetti A. CFD combustion and emission formation modeling for a HSDI diesel engine using detailed chemistry. In: ASME 2006 Internal Combustion Engine Division Fall Technical Conference; Sacramento, California; 5-8 November 2006; http://dx.doi.org/10.1115/ICEF2006-1506.

[19] Mattarelli E, Rinaldini, CA, Cantore G. CFD optimization of a 2-stroke range extender engine. International Journal of Automotive Technology 2015; 16 (3): 351-69. http://dx.doi.org/10.1007/s12239-015-0037-y.

[20] Rinaldini CA, Mattarelli E, Golovitchev VI. Potential of the Miller cycle on a HSDI diesel automotive engine. (2013) Applied Energy 2013;112:102-19. http://dx.doi.org/10.1016/j.apenergy.2013.05.056.

[21] Golovitchev VI, Nordin N, Jarnicki R, Chomiak J. 3D Diesel Spray Simulation Using a New Detailed Chemistry Turbulent Combustion Model. SAE Technical Paper 2000; No. 2000-01-1891. https://doi.org/10.4271/2000-01-1891.

[22] Golovitchev VI, Imren A. Development of Dual Fuel Combustion Models for Direct Injected Heavy Duty Diesel Engines. In: Silva C, Riveira A, editors. Diesel Fuels: Characteristics, Performances and Environmental Impacts, New York:Nova Publisher; 2013

[23] Ehleskog, R, Golovitchev V, Denbratt I, Andersson S, Rinaldini CA. Experimental and numerical investigation of split injections at low load in an HDDI diesel engine equipped with a piezo injector. SAE Technical Papers 2006; No. 2006-01- 3433. https://doi.org/10.4271/2006-01- 3433.